Chemical Engineering Journal 152 (2009) 530–536

Contents lists available at ScienceDirect

Chemical Engineering Journal

journal homepage: www.elsevier.com/locate/cej

Effect of fibres on fluidized bed expansion parameters

Eric Loranger, Mélissa Canonne, Claude Daneault[1], Bruno Chabot*

Centre intégré en pâtes et papiers, Université du Québec à Trois-Rivières, 3351 boul. des Forges, C.P. 500, Trois-Rivières, QC G9A 5H7, Canada

ARTICLE INFO

Article history:
Received 19 February 2009
Received in revised form 11 May 2009
Accepted 17 May 2009

Keywords:
Fluidized bed
Fibres
Flocculation
Adsorption
Dissolved and colloidal substances
Crowding factor

ABSTRACT

Better ways to protect water resources and the environment must be implemented in the papermaking industry to help Canada achieve its strategic target in maintaining a healthy environment and ecosystems. Closing down paper machine whitewater systems is the only way to reach that goal. However, under such conditions, a build-up of dissolved and colloidal substances in whitewater occurs. This results in lower paper quality and paper machine runnability problems. A fluidized bed reactor with modified solid sorbents is proposed to remove contaminants from paper machine whitewater prior to recycling. However, the whitewater fibre content significantly modifies bed expansion creating a major impact on the terminal particle velocity and the Richardson and Zaki expansion coefficient. Fibre flocculation was identified as a key characteristic that must be included in the classical equations describing fluidization. A modification for Newton's terminal velocity law and a new model for the expansion coefficient have been developed.

1. Introduction

Papermaking is an industrial process using very large amounts of water. It also produces significant volumes of wastewater containing various amounts of pollutants. Although significant efforts have been made to reduce detrimental effects on the environment and ecosystems, the current growing economy/population will increase the competition between humans and other species for natural resources, especially water [1]. As water needs are increasing, the pressure to recycle and reuse water will increase. Therefore, further efforts by the papermaking industry will be required to help Canada achieve its strategic target in maintaining a healthy environment and ecosystems. One way to achieve that goal is to force paper mills to further reduce their fresh water consumption and reject loads by increasing whitewater system closure. However, a significant build-up of contaminants in process water will occur under those process conditions [2]. Moreover, economical considerations and virgin fibre supply limitations adopted by the government of Quebec [3] are also promoting the use of recycled pulp, although they are considered an important source of contaminants. Both issues will then contribute to an excessive build-up of dissolved and colloidal substances (DCS) in whitewater leading to serious production problems or paper quality issues [4].

In order to overcome the excessive accumulation of contaminants in paper machine whitewater under highly closed systems, we are proposing a method to remove them by selective adsorption on modified solid sorbents (beads). The choice of contact technique must account for the presence of valuable cellulose particles (fibres and fines) and their clogging potential. A fluidized bed reactor provides efficient contact while enabling the recovery of fibres and fines. This technology has successfully been used in many applications to remove heavy metal ions [5,6], humic acid [7] and proteins [8]. However, those studies were carried out with liquids not containing any solid particles such as wood fibres.

A liquid fluidized system is characterized by a regular expansion of the bed of solid particles as the velocity of the liquid increases from the minimum fluidization velocity to the terminal velocity of the particles. For sedimentation or fluidization of uniform particles, Richardson and Zaki [9] showed that bed expansion is described by Eq. (1). The expansion coefficient (n) can be calculated using numerous correlations [9–11]; the most recent being by Khan and Richardson [12]. Terminal velocity (V_T) can be determined by a second correlation from Khan and Richardson [13] or with more classical equations from Stokes, Newton [14] or Van Allen. Newton's terminal velocity relation is expressed by Eq. (2). Typical equations used for predicting terminal velocity involve the terminal Reynolds number and the Galileo number. The Reynolds number is related to the flow regime while the Galileo number is related to the physical characteristics of the beads (density and diameter) and fluid properties (density and viscosity).

$$\frac{V_i}{V_T} = \varepsilon^n \tag{1}$$

$$Re_T = (3Ga)^{0.5} \tag{2}$$

* Corresponding author. Tel.: +1 819 376 5011/4510; fax: +1 819 376 5148.
E-mail address: Bruno.Chabot@uqtr.ca (B. Chabot).
[1] Canada Research Chair in Value-added Paper.

1385-8947/$ – see front matter © 2009 Elsevier B.V. All rights reserved.
doi:10.1016/j.cej.2009.05.022

Nomenclature

A_R	reactor cross-section area (m^2)
C_m	mass consistency (%)
D_B	bead diameter (m)
g	gravitational acceleration (m/s^2)
Ga	Galileo number, $D_B^3\rho_F(\rho_B - \rho_F)g/\mu^2$
H	bed height (m)
H_0	initial bed height (m)
L	fibre length (m)
L_A	arithmetic average fibre length (m)
L_w	weighted average fibre length (m)
M_B	total bead mass (kg)
n	expansion coefficient
N	crowding number based on the arithmetic average fibre length
N_w	crowding number based on the weighted average fibre length
Q_i	incoming fluid flow rate (m^3/s)
Re_T	Reynolds number, $\rho_F V_T D_B/\mu$
V_B	occupied volume of the beads, M_B/ρ_B (m^3)
V_i	superficial liquid velocity (m/s)
V_R	total reactor volume, $A_R H$, $V_B + V_V$ (m^3)
V_T	terminal velocity of the particles (m/s)
V_V	void volume (m^3)

Greek symbols

ρ_B	bead density (kg/m^3)
ρ_F	fluid density (kg/m^3)
ε	void fraction
ω	fibre coarseness (kg/m)
μ	fluid viscosity (kg/(m s))

From these parameters, Eq. (1) is used to predict the void fraction or bed height at any fluid velocity. These equations are valid for perfectly spherical particles and for pure liquids. Therefore, they cannot be applied in our case due to the presence of numerous solid particles (fibres and fines) that are expected to affect the bed expansion during fluidization. Therefore, bed expansion behaviour with such process water should include fibre and pulp suspension properties, and especially the flocculation phenomena of pulp. As in many papermaking processes, our study involves pulp suspensions where fibre flocculation is a critical phenomenon that must be taken into account in the fluidization process. In an effort to characterize the fibre flocculation phenomenon, Kerekes and Schell [15] have defined a crowding factor. The crowding factor or number (N) is given by Eq. (3). This parameter represents the number of fibres in a spherical volume with a diameter equal to the length of a fibre and accounts for fibre morphology (length and coarseness) as well as fibre concentration.

$$N = \frac{5C_m L^2}{\omega} \tag{3}$$

Kerekes and Schell [15] showed a direct correlation between the crowding factor and the number of contacts per fibre, thus describing flocculation. The higher the crowding number is, the higher the pulp flocculation potential. Assuming that a floc is an aggregate of a minimum of 3 fibres, the corresponding crowding factor value is 60. In order to calculate the crowding number, we need to determine the fibre length. However, a pulp's fibre length is not uniform but is rather a statistical distribution of various fibre lengths. Huber et al. [16] established a new definition for the crowding factor in terms of spherical volume probability and value. With the integration over the fibre length range, the multiplication of the probability function by the spherical volume distribution gives the mean crowding number. The mathematical parameters added in their study have greatly complicated the determination of the formula, but they also showed that the use of the weighted average fibre length (L_w) with the Kerekes and Schell formula produces good results while keeping the crowding factor determination simple. The crowding number based on the weighted average fibre length is noted as N_w. As in the case of the crowding number, consistency is also closely related to floc strength [17]. The Young elastic modulus, the length to diameter ratio of the fibres and the liquid turbulence also play a significant role [17]. Depending on turbulence conditions, transient and coherent flocs can be found in pulp suspensions [18]. For the same pulp properties, low or decaying turbulence will increase floc size and strength compared to high turbulence areas [19,20].

In summary, the presence of fibres through fibre flocculation and/or floc strength may play a significant role on bed expansion behaviour. The objective of this study is to assess the effect of pulp suspension characteristics on the parameters used by Richardson and Zaki to describe a fluidized bed, namely the expansion coefficient (n) and the terminal velocity (V_T).

2. Materials and methods

2.1. Materials

2.1.1. Pulp and beads

Soda-lime glass (Fisher Scientific), acrylic and stainless steel beads (Salem Ball) of 3 and 4 mm in diameter were selected as model particles for fluidization experiments as they cover a wide density spectrum. Beads were characterized and their properties are presented in Table 1. Bead diameter was determined with a digital calliper meter (Starrett 797B) with a resolution of 0.01 mm. Ten beads were arbitrarily chosen and measured once. In order to determine the sphericity of the bead, the diameter of a single bead was measured in 10 different axes. The bead diameter was then calculated from the average values. Beads density was calculated by weighting 10, 20, 30, 40 and 50 beads on a four-digit precision balance (Mettler Toledo AG245). The individual weight of a bead was then calculated from the slope of a linear regression between total weight and bead count. From the mean diameter, the average bead volume was determined which was used to calculate the bead density for each material.

Pulp from different pulping processes was selected to obtain different fibre lengths from the same wood species. A typical newsprint whitewater sample was also tested and included in the modeling for comparison purposes. Stone groundwood (SGW), thermomechanical (TMP), Kraft pulp and the newsprint whitewater (WW) samples were supplied by an Eastern Canadian paper mill. Pulp and whitewater properties are presented in Table 2. Average weighted length and coarseness are required to calculate the crowding factor as discussed in Section 1.

2.1.2. Experimental apparatus

Terminal velocity measurements were carried out using the apparatus presented in the schematic in Fig. 1.

Table 1
Bead characteristics.

	Diameter (mm)	Density (kg/m^3)
3 mm acrylic	3.00 ± 0.01	1196 ± 4.7
4 mm acrylic	3.96 ± 0.01	
3 mm soda-lime glass	2.93 ± 0.04	2616 ± 30.1
4 mm soda-lime glass	3.96 ± 0.03	
3 mm stainless steel	2.99 ± 0.01	8044 ± 4.1
4 mm stainless steel	3.99 ± 0.01	

Table 2
Pulp properties.

	SGW	TMP	Kraft	WW
Arithmetic average fibre length, L_A (mm)	0.28	0.66	1.21	0.16
Length-weighted fibre length, L_w (mm)	0.63	1.56	2.22	0.33
Fines content (%)	62.1	33.8	25.4	84.5
Coarseness (mg/100 m)	18.9	22.8	15.3	22.8

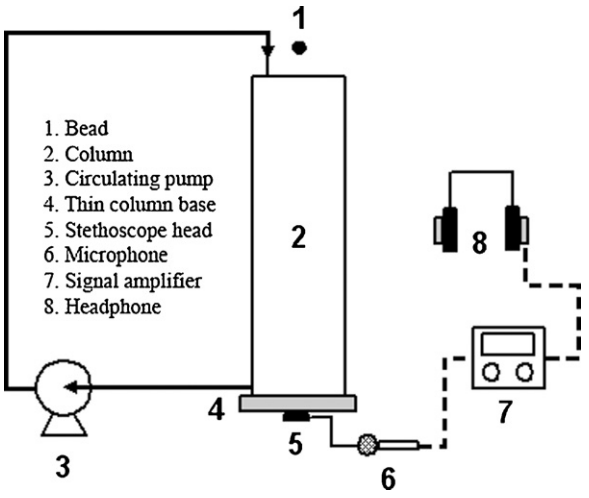

Fig. 1. Schematic diagram of the experimental apparatus for terminal velocity measurement.

The terminal velocity of the bead (1) was determined by measuring the time required for a bead to flow down a 1.5 m long column of 6.16 cm in diameter (2). Due to the presence of fibres in the fluid, it was impossible to follow the bead flowing down the column. Therefore, a sound detector was used to determine the time for the bead to reach the bottom of the column. The very thin column base (4) was fitted with a stethoscope (5) that carried a sound wave to a microphone (6) through a short flexible tube of 1.9 cm in diameter. The electric signal from the microphone was then amplified (7) to a set of headphones (8) to help the operator hear the sound of the bead impacting the bottom. The addition of a circulating pump (3) was required since pulp flocculates and settles to the bottom.

Bed expansion trials were carried out with a fluidized bed experimental setup shown in the schematic in Fig. 2.

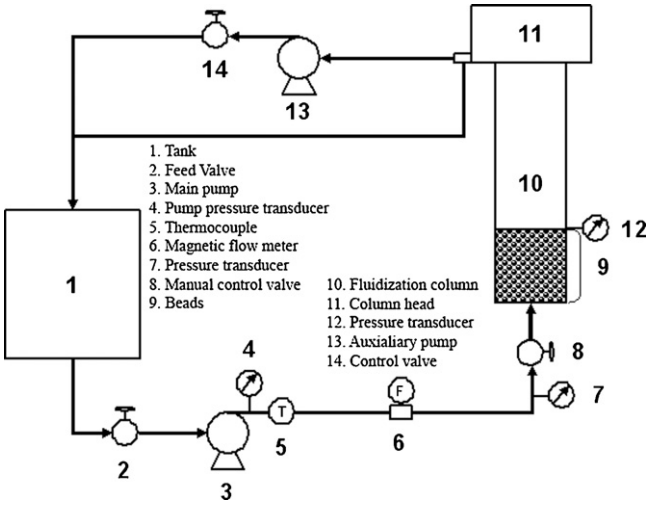

Fig. 2. Schematic diagram of the experimental fluidized bed reactor.

Table 3
Factorial design.

	Consistency (%)			
	SGW	TMP	Kraft	WW
3 mm acrylic 4 mm acrylic 3 mm soda-lime glass 4 mm soda-lime glass 3 mm stainless steel 4 mm stainless steel	0 (water), 0.05, 0.1 and 0.2			0.32

The pump (2), from Grundfos (model JPS4-A), draws the feed pulp suspension from the tank which is equipped with a 1200 W heater. The water exits at the top of the column to the manual control valve (8). The fluidization column (10) is made of transparent polyvinyl chloride (PVC) (6.16 cm inner diameter and 1.25 m in length). A graduated tape positioned on the outside surface of the fluidization column is used to determine bed expansion during fluidization trials. The beads (9) are initially packed in the bottom of the column. The head of the reactor (11) is filled up by the overflow from the reactor vessel. The head is then drained using gravity for a low flow rate or by a second pump (13) (Grundfos, model JPS4-A) through the control valve (14) for a high flow rate. Signals from a type J thermocouple (5) (Omega Engineering), from PX-181 pressure transducers (4, 7, 12) (Omega Engineering), and from a magnetic flow meter (6) (ABB) are all fed to a personal computer equipped with a proper data acquisition card (DAS-801) (Omega Engineering). A homemade Visual basic program has been developed to record temperature, pressure and flow for each experiment. Sampling time was 5 s and the total duration of each data point was 2 min. The bed height was recorded 3 times during this time. All the measuring equipment has an accuracy lower than 0.5% and the error on the bed height is 0.5 mm. This experimental setup has been designed for liquid flow rate ranging from 0 to 70 L/min and for bead weights of up to 1.5 kg.

2.2. Methods

2.2.1. Pulp suspensions

Over the years, the Technical Association of the Pulp and Paper Industry (TAPPI) has been standardizing the various methods used by papermakers. This association is very similar to the American Society for Testing and Material (ASTM) but for the pulp and paper industry. Accordingly, pulp slurries were prepared as described in TAPPI standard method T-262. Fibre length and coarseness were determined using a Fibre Quality Analyzer (FQA) according to TAPPI standard method T-271. Pulp slurries were allowed to stabilize at room temperature (25 °C) prior to terminal velocity and bed expansion experiments.

2.2.2. Factorial design

A factorial design was used to study the effect of various bead types and sizes for SGW, TMP, Kraft and newsprint whitewater at several pulp slurry consistencies (Table 3) chosen with respect to typical industrial values. For example, 3 mm glass beads were subjected to 3 pulps (SGW, TMP and Kraft) at 4 consistencies (0, 0.05, 0.1 and 0.2%) and to WW at 0.32% consistency. Consistency is defined as the weight percentage of oven-dry fibre over the total weight of the pulp suspension. As discussed previously, Kerekes and Schell defined a crowding number to characterize the pulp suspension flocculation potential [15] as a function of pulp consistency and fibre length. In our case, the crowding factor ranged from 0.5 to 2.1 for SGW, 2.7–10.7 for TMP, 8.1–32.4 for Kraft and 0.8 for the newsprint whitewater.

2.2.3. Terminal velocity

Terminal velocity was determined with the apparatus described previously (Fig. 1). The time required for a bead to travel from the top to the bottom of the column was determined using a stopwatch with a precision of 1/100th of a second. The stopwatch was started when the bead was released by the operator and stopped when a hit was detected. Each pulp–bead combination was repeated 30 times to estimate the standard deviation. To ensure good dispersion and homogeneity of the pulp in the column, the pulp suspension was circulated using the pump for 1 min before dropping the bead. The average of the 30 measurements was reported as the terminal velocity.

2.2.4. Expansion curves

Expansion curves were determined using the fluidized column filled with 1.5 kg of the appropriate beads and the initial bed height was recorded for reference. The experiments were carried out with tap water adjusted to the desired temperature (25 °C) as a control and with pulp at the selected consistency. Expansion curves were constructed by adjusting the flow rate to a desired value, and then recording the height of the bed with the graduated tape on the reactor vessel. Three trials were carried out for each experimental condition to estimate the variability of the test (standard deviation).

3. Results and discussion

3.1. Bed expansion curves

3.1.1. Determination of the standard deviation

The bed expansion curves for 4 mm soda-lime glass beads with tap water and Kraft fibres at the highest consistency (0.2%) are reported in Fig. 3. As stated in the methodology, each condition was repeated 3 times (circle, square and triangle markers). Results clearly show that expansion curves are very reproducible and exhibit very low variability as shown by the small error bars for each data point. The maximum deviation for the flow rate is 2.8% and 4.1% for the relative bed height, even with Kraft pulp at the highest consistency (0.2%). Relative bed height values are reported for comparison purposes. Since beads have different densities, for the same mass, different initial bed height values are measured.

3.1.2. Fluidization with pulp suspensions

Results show that the bed expansion is strongly dependent on bead density and diameter. As density rises, the flow rate required to achieve a given bed expansion increases. A 100% bed expansion (relative height) with water (25 °C) for 3 mm acrylic beads requires

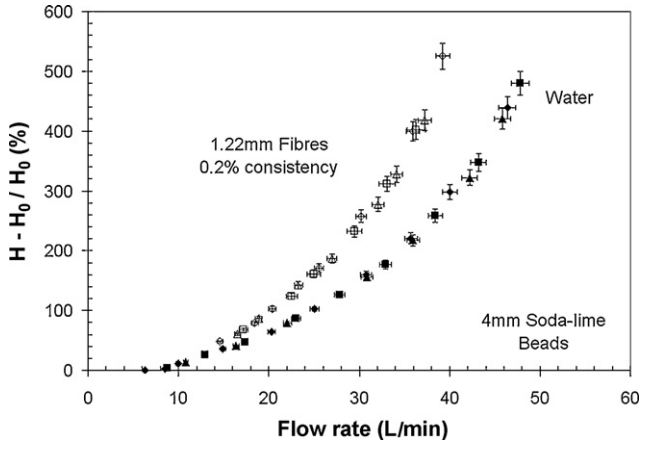

Fig. 3. Standard deviations for bed expansion trials with 4 mm glass beads for water and a Kraft pulp suspension at 0.2% consistency.

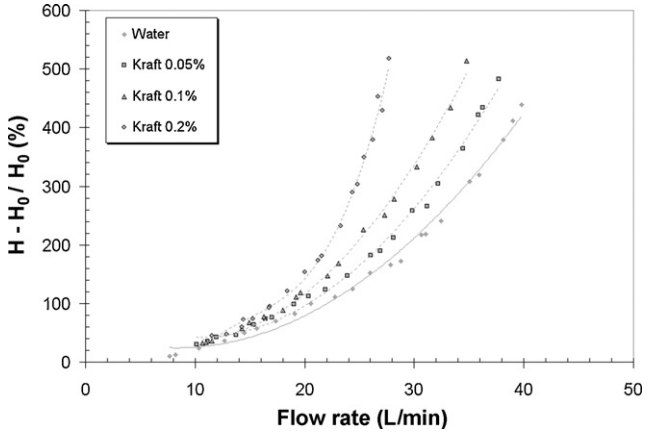

Fig. 4. Bed expansions with Kraft pulp slurries for 3 mm soda-lime glass beads at 25 °C.

a lower flow rate (6 L/min) than 3 mm soda-lime glass (21.2 L/min) and 3 mm stainless steel beads (43.5 L/min). As the bead diameter increases, the flow rate required for a given bed height also increases. For example, 100% bed expansion with water (25 °C) for 4 mm acrylic beads was achieved at a flow rate of 7.4 L/min, 24.7 L/min for 4 mm soda-lime glass and 49.5 L/min for 4 mm stainless steel beads.

Fig. 4 presents a typical bed expansion curve showing the effect of flow rate and Kraft pulp suspension consistency for 3 mm soda-lime glass beads. Results indicate the presence of two different flow regimes ranging around 15 L/min. At low flow rates (<15 L/min), Kraft pulp suspensions behaved much like water, while at higher flow rates (>15 L/min), the bed expansion increased with pulp consistency. This could be most likely attributable to fibre flocculation and floc strength. At low flow rates (<15 L/min), the bed is not fully expanded and the beads are more closely packed (low ε), thus creating a larger restriction to the flow of the pulp suspension (higher pressure drop). Even if the flow rate is low, flocs formed below the bed (inlet) are probably broken apart due to collision with the beads. Very small and strong transient flocs or individual fibres can thus flow through the bed without any significant contribution in lifting the beads. At higher flow rates, the bed is expanded with much more space between the beads (high ε). It has also been noticed that the upper part of the bed is stretched, thus resulting in a void fraction gradient from bottom to top. Since the bed is expanding in the column, it leaves more time and space for fibres to reflocculate as they travel towards the top of the column [19]. Moreover, the turbulence level from the bottom to the top of the column decays leading to the formation of larger and stronger flocs [20]. This phenomenon most likely contributes in lifting the beads during fluidization, much like a screen mesh and could explain the void fraction gradient observed, resulting in stronger exponential profiles for slurries at higher consistencies.

Results for other pulp–bead combinations (data not shown) are in agreement with the hypothesis that fibre flocculation and floc strength are key parameters in the expansion of beads with fibre suspensions. Lower flocculation potential or crowding number, from lower consistency or shorter fibres, gives a lower exponential profile and a lower bed height for any given flow rate. Therefore, the classic fluidization behaviour mentioned earlier with regard to bead density and diameter apply.

3.2. Terminal velocity in pulp suspensions

3.2.1. Measurements

Fig. 5 presents the effect of Kraft slurry consistency, bead diameter and density on the terminal velocity. Unfortunately, no data

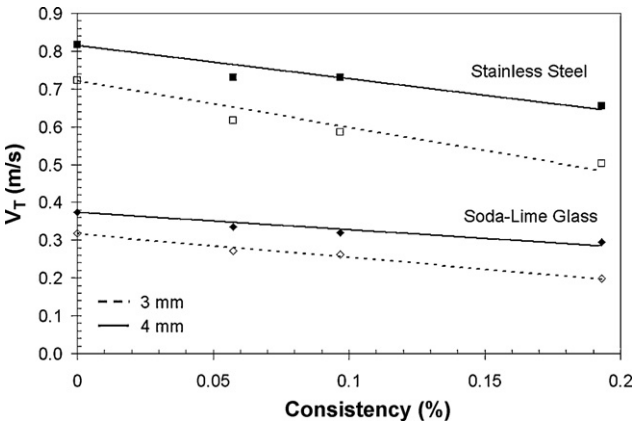

Fig. 5. Terminal velocity with a Kraft pulp slurry for 3 and 4 mm beads at 25 °C.

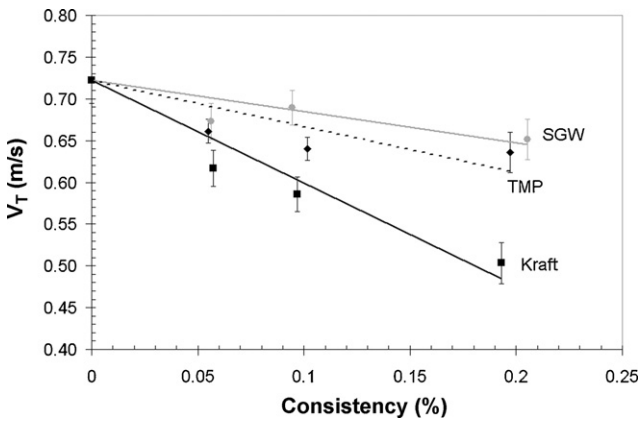

Fig. 6. Terminal velocity for 3 mm stainless steel and various pulp slurries at 25 °C.

were reported with acrylic beads since it was impossible to clearly determine the impact of the bead at the bottom of the column. However, visual measurement was achieved in water and used as additional data for terminal velocity modeling (Section 3.2.2).

As shown in Fig. 5, increasing the pulp consistency reduces the terminal velocity whatever bead diameter or density studied. Moreover, increasing the bead density increases the effect of consistency on terminal velocity. With respect to both diameters, the negative slope for stainless steel beads is about twice that of soda-lime glass beads. For the same bead density, the slope of the 3 mm beads is about 27% more negative than the slope for the 4 mm stainless steel or soda-lime glass beads. Thus, the maximum fibre impact is achieved for 3 mm stainless steel beads. It has been reported in literature [21] that if large and small particles are settling at low Reynolds numbers, the path of both particles will not be in a straight line but rather curved. Basically, the turbulence generated by one particle interacts with the other even when the particles are not close enough to touch each other. As a result, both particles settle faster than single particles alone. The same analogy may apply in our case, if fibre flocs and beads are considered as two particles. The soda-lime glass beads settle at low Reynolds numbers while stainless steel beads settle at high Reynolds numbers. Under the latter conditions, the particles settle down in a straighter path and are not accelerated by the flocs, but rather slowed down as they hit fibre flocs during sedimentation. This explanation is in agreement with results observed for stainless steel beads which exhibit a stronger terminal velocity reduction than soda-lime glass beads.

In summary, stainless steel beads dissipate more energy when contacting fibre flocs resulting in a straighter falling path. The curved falling path for soda-lime beads may reduce the quality and the quantity of contacts, thus dissipating less energy.

In order to assess the effect of consistency on various pulp or fibre lengths, Fig. 6 shows the result of terminal velocity for 3 mm stainless steel and various pulp slurries. Results show that Kraft slurries exhibit a stronger effect on terminal velocity. This was expected since the flocculation potential (crowding factor) of Kraft pulp is higher, resulting in stronger flocs, thus having a higher interference with the beads. SGW and TMP pulp curves are similar but TMP slurries seem slightly lower. For all the beads (data not shown), the terminal velocity reduction was found to follow the flocculation potential order.

As time elapses, the pulp starts to flocculate, depending on the crowding factor, and begins to settle. It has been reported [22] that the overall solid flux toward the bottom is compensated by an upward flow of fluid, increasing turbulence within the liquid. This increase in turbulence could easily increase the drag force on the bead and reduce their terminal velocity when they are dropped in a slowly flocculating and settling pulp.

3.2.2. Terminal velocity modeling

In order to be able to predict the terminal velocity for various pulp and bead characteristics, multiple linear regression analysis using a statistical modeling software (SAS JMP 7.0) was used to determine the key variables. As presented in Eq. (2), the terminal velocity is expressed from the Galileo number and stands only for pure liquids. The linearization of Newton's equation leads to Eq. (4).

$$\ln(Re_T) = 0.5\ \ln(3Ga) \tag{4}$$

The effect of the fibre was studied using pulp properties, namely consistency, fibre length, fines content and the crowding factor as well as fluidization variables (bead diameter and density, Galileo number and Reynolds number). Second order interactions for all combinations were analyzed but found to be insignificant. At a 95% confidence limit, the key modeling variables for the terminal velocity were the Galileo number and the crowding factor. Therefore, the crowding factor (N_w) was introduced in the equation in the form of $\ln(1+N_w)$. This term was used to remove the mathematical discrepancy resulting for the following case: if N_w is equal to 0 (for water alone), $\ln(1+N_w)$ gives 0 instead of the indetermination resulting from ln(0). The final model correlation, based on multiple linear regressions of the linearized variables, is given by Eq. (5).

$$Re_T = 0.8834(3Ga)^{0.5}(1+N_w)^{-0.0766} \tag{5}$$

The pre-exponential factor (0.8834) and the exponent term for the Galileo number (0.5) were validated by the linear regression of Re_T vs. $3Ga$ (not shown) with water data. Thus the terminal velocities measured are 88.3% of the values predicted by Newton's law, giving an 11.7% deviation. Experimental deviations from Newton's settling law were also reported elsewhere in literature [23]. This study showed that the actual limitation of the equation was the assumed linearity of the falling path, the near perfect sphericity of the beads and a low fluid turbulence. Any deviation from these assumptions will reduce the actual terminal velocity from Newton's predicted value. The factor is therefore a correction of Newton's law for our system and is not associated with the fibre effect, thus reinforcing the utility of the crowding factor. Therefore, Eq. (5) predicts the experimental results with great accuracy as shown in Fig. 7. Eq. (5) should be used within the limitation of the experiments, i.e. $6.5\times10^4 < Ga < 7.9\times10^6$ and $0 < N_w < 33.4$ for a Re_T in the range of 390–4150, since the validity was not tested beyond theses values.

3.3. Expansion coefficient in pulp suspensions

3.3.1. Measurements

As stated in the Richardson and Zaki equation, the expansion coefficient plays a very significant role in describing the exponential trend of bed expansion. However, the void fraction is rather difficult

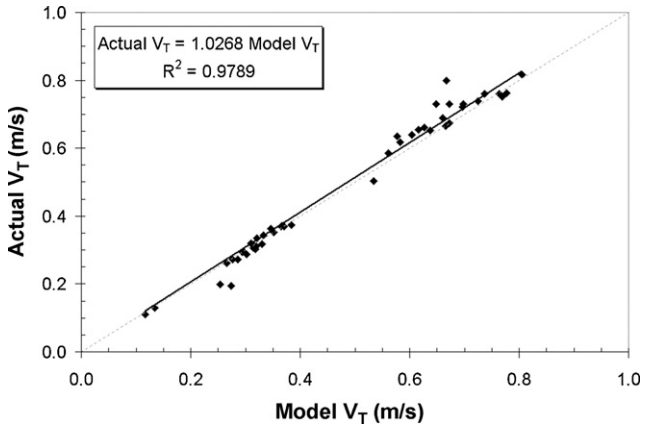

Fig. 7. Actual vs. model of predicted terminal velocity for all the bead–pulp combinations at 25 °C.

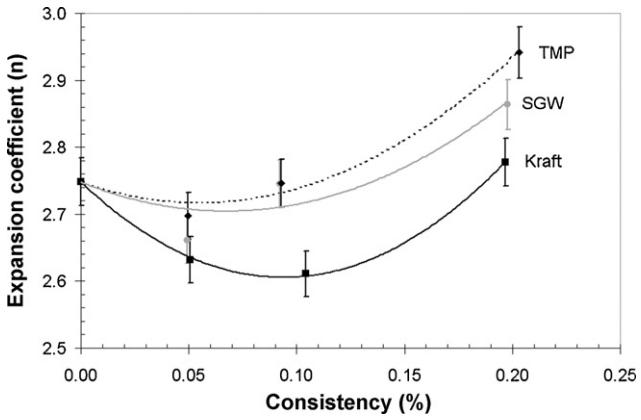

Fig. 9. Expansion coefficient for 3 mm soda-lime glass and various pulp slurries at 25 °C.

to measure requiring specialized equipment such as conductivity electrodes [24] or X-ray sources [25].

The bed height was thus measured and the void fraction calculated. For a known mass and density of beads, we can easily estimate the volume it occupies (V_B). From the bed height (H) and the column cross-sectional area (A_R), we can determine the total volume of the column (V_R). The void volume (V_V) is then calculated by subtracting V_R from V_B. The void fraction (ε) is now reported as the ratio V_V/V_R. This calculation method was based on the assumption that the void fraction is homogeneously distributed throughout the column. However, we know that bed stretching occurs during fluidization at high pulp consistency and care must be taken in the analysis of the void fraction. The liquid velocity (V_i) was calculated from the ratio of the incoming flow rate (Q_i) to the reactor cross-sectional area (A_R). The data was fitted by linear regression to a linearized form of Richardson and Zaki (Eq. (6)).

$$\ln(V_i) = \ln(V_T) + n\ \ln(\varepsilon) \tag{6}$$

As described in the Di Felice study [22], terminal velocity values estimated from Richardson and Zaki using our data was found to be smaller than the actual experimental values (not shown). In an effort to reduce this deviation, the intercept of each linear regression in Eq. (6) was forced to the terminal velocity value previously obtained. The expansion coefficient was then associated to the slope of the corrected linear regression. The experimental error for the slope determination was small in the case of the soda-lime glass (about 1.4%) while larger for stainless steel beads (about 5.6%). Fig. 8 shows the results obtained for Kraft pulp slurries and various bead types. The expansion coefficient with regards to consistency exhibits a quadratic trend for every type of bead studied.

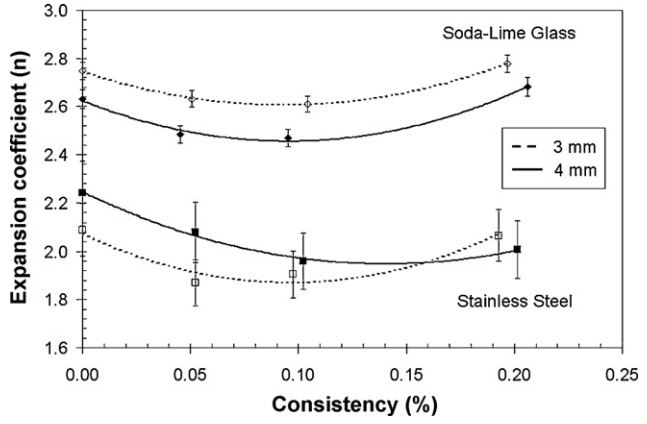

Fig. 8. Expansion coefficient with a Kraft pulp slurry for 3 and 4 mm beads at 25 °C.

The expansion coefficient reaches a minimum at 0.1% consistency while the 0.2% value is very similar to water. The presence of a minima was also reported in another study where the expansion coefficient was plotted against biofilm thickness on inert particles [26] but no insight was given.

However, taking into account the experimental error, stainless steel curves are not statistically different from each other while the soda-lime glass curves are different. At a given consistency, an increase in bead density reduces the value of n and in the case of the soda-lime glass beads; an increase in bead diameter also results in a reduction in the value of n. These results agree with a study from Baldock et al. [27] for both variables. In order to investigate the effect of fibre length, data from the 3 mm soda-lime glass beads were plotted in Fig. 9.

We can conclude that TMP and SGW pulps behave similarly. Both pulps exhibit a small decrease in their terminal velocity as shown in Fig. 6. A similar trend has been found for soda-lime glass beads (data not shown). Both types of pulp also have a small crowding factor, thus low flocculation potential and less bed stretching resulting in a void fraction similar to water. According to Eq. (1), if the decrease of V_T is small and the increase for ε is limited, then any increase in V_i must be accounted for in the n value. However, Kraft pulp does not appear to follow this trend. The Kraft curve reaches a minimum at 0.1% with a stronger quadratic trend in comparison to SGW or TMP. Kraft pulp exhibits a high terminal velocity drop, high bed stretching, and thus a high ε variation. The mathematical concern with Eq. (1), expressed previously, is slightly transformed as the decrease of V_T and the increase of ε are significant. The expansion coefficient may thus have a lesser effect. This effect seems to be directly related to the crowding factor or flocculation potential since a more flocculated pulp increases the stretching phenomena of the bed, thus increasing the void fraction.

All the data from experiments (not shown) is in agreement with Figs. 8 and 9 showing the same quadratic trend but with a different magnitude. The 4 mm soda-lime curve is very similar to Fig. 9 but with lower values. For stainless steel beads, the fibre length effect observed for soda-lime glass shown in Fig. 9 was not found. In the case of stainless steel beads, the three curves are almost identical (data not shown). The bead density seems to have a significant effect on this behaviour and needs further investigation in order to be fully understood. For a given consistency, 3 mm stainless steel bead values are slightly higher than 4 mm beads but very close to the experimental error.

3.3.2. Expansion coefficient modeling

To predict the coefficient value of a fluidized bed with various types of pulp, multiple linear regression analysis was also used.

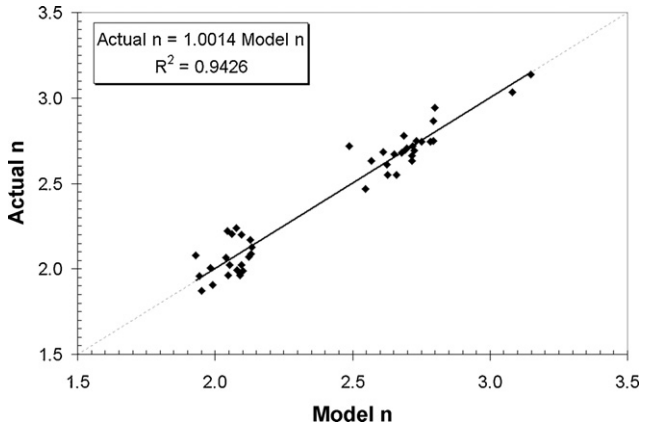

Fig. 10. Actual vs. model of predicted expansion coefficient for all the bead–pulp combinations at 25 °C.

From the statistical analysis with a 95% confidence limit, bead density, fibre length, Galileo number and the crowding factor were identified as key variables for the expansion coefficient. For the specific Reynolds number range targeted, unlike the terminal velocity case, the expansion coefficient is not given by an equation but rather by a constant value of 4.65 [9]. This value is clearly in disagreement with our experimental data. Therefore, a new correlation based on the key variables identified was developed (Eq. (7)). Our experimental data were fitted with a high correlation coefficient (R^2) of 0.94.

$$\ln(n) = 1.518 - 4.198 \times 10^{-5}\rho_B - 132.6L - 2.901 \times 10^{-2}\ln(Ga) + 3.568 \times 10^{-2}\ln(1 + N_w) \quad (7)$$

The parity plot of Fig. 10 shows a very good prediction capability for Eq. (7), within our experimental conditions, i.e. $6.5 \times 10^4 < Ga < 7.9 \times 10^6$, $0 < N_w < 33.4$, $1200 < \rho_B < 8000\,kg/m^3$ and $0 < L < 1.22$ mm with n in the range of 1.75–3.2. On the whole range of experiments, the maximum error reported is 9% while the mean error is 0.1%. Combining Eqs. (5) and (7), we can now predict the expansion of a bed of various beads in the presence of various types of fibre. Both parameters (n and V_T) are affected by the presence of fibres or their flocculation characteristics and this implies a correction to the usual Richardson and Zaki equation used in a fluidized bed reactor.

4. Conclusions

The purpose of this work was to determine the effect of fibres on the n and V_T parameters used in the Richardson and Zaki equation to describe a fluidized bed expansion.

The following are the major findings of this study:

(1) Flocculation of the pulp during fluidization was found to exert a very significant effect on bed expansion, especially at flow rates higher than 15 L/min. The pulp flocs act like a screen mesh and will drag the bead along in the fluidization column, thus stretching the height of the bed.
(2) The terminal velocity of the beads was accurately predicted, within the experimental conditions, by a modified Newton law including a term for the crowding factor (Eq. (5)). Deviation from Newton's law reported in the literature for water was also observed in our experiments.
(3) The expansion coefficient was also accurately described in the presence of fibres and the key variables were identified as bead density, fibre length, Galileo number and crowding factor. The variables were used to develop Eq. (7) which fits the data with very good accuracy within the experimental conditions.

Acknowledgements

The authors gratefully acknowledge the Canada Research Chair in Value-added Paper and NSERC for their financial support.

References

[1] Environment Canada, Threats to water availability in Canada, NWRI Scientific Assessment Report Series No. 3, National Water Research Institute, Burlington, Ontario, 2004.
[2] A. Geller, L. Gottsching, Closing water systems completely in the Federal Republic of Germany, Tappi J. 65 (1982) 97–101.
[3] G. Coulombe, J. Huot, J. Arseneault, E. Bauce, J.-T. Bernard, A. Bouchard, M.A. Liboiron, G. Szaraz, Commission d'étude sur la gestion de la forêt publique québécoise, Bibliothèque nationale du Québec, 2004 (in French).
[4] F. Linhart, W.J. Auhorn, H.J. Degen, R. Lorz, Anionic trash: controlling detrimental substances, Tappi J. 70 (1987) 79–85.
[5] P. Zhou, J.-C. Huang, A.W.F. Li, S. Wei, Heavy metal removal from wastewater in fluidized bed reactor, Water Resour. 33 (1999) 1918–1924.
[6] C. Lee, W. Yang, C. Hsieh, Removal of copper (II) by manganese-coated sand in a liquid fluidized-bed reactor, J. Hazard. Mater. B114 (2004) 45–51.
[7] E.K. Kim, H.W. Walker, Effect of cationic polymer additives on the adsorption of humic acid onto iron oxide particles, Colloids Surf. A 194 (2001) 123–131.
[8] Q. Lan, A. Bassi, J. Zhu, A. Margaritis, Continuous protein recovery from whey using liquid–solid circulating fluidized bed ion-exchange extraction, Biotechnol. Bioeng. 78 (2002) 157–163.
[9] J.F. Richardson, W.N. Zaki, Sedimentation and fluidisation. Part 1, Trans. Inst. Chem. Eng. 32 (1954) 35–53.
[10] P.N. Rowe, A convenient empirical equation for estimation of the Richardson–Zaki exponent, Chem. Eng. Sci. 43 (1987) 2795–2796.
[11] J. Garside, M.R. Al-Dibouni, Velocity–voidage relationships for fluidization and sedimentation in solid–liquid systems, Ind. Eng. Chem. Process Des. Dev. 16 (1977) 206–213.
[12] A.R. Khan, J.F. Richardson, Fluid–particle interactions and flow characteristics of fluidized beds and settling suspensions of spherical particles, Chem. Eng. Commun. 78 (1989) 111–130.
[13] A.R. Khan, J.F. Richardson, The resistance to motion of a solid sphere in a fluid, Chem. Eng. Commun. 62 (1987) 135–150.
[14] I. Newton, Principia Book II, Prop. XXXIX, Theor. XXXI (1687).
[15] R.J. Kerekes, C.J. Schell, Characterization of fibre flocculation regimes by crowding factor, J. Pulp Paper Sci. 18 (1992) 32–38.
[16] P. Huber, J.-C. Roux, E. Mauret, N. Belgacem, C. Pierre, Suspension crowding for a general fibre-length distribution: application to flocculation of mixtures of short and long papermaking fibres, J. Pulp Paper Sci. 29 (2003) 77–84.
[17] N. Thalen, D. Wahren, An experimental investigation of the shear modulus of model fibre networks, Svensk Pappersitd. 67 (1964) 474–480.
[18] A.A. Robertson, S.G. Mason, Flocculation in flowing pulp suspensions, Pulp Paper Mag. Can. 55 (1954) 263–269 (Convention Issue).
[19] S.G. Mason, Fibre motion and flocculation, Tappi J. 37 (1954) 494–501.
[20] R.J. Kerekes, Pulp flocculation in decaying turbulence: a literature review, J. Pulp Paper Sci. 9 (1983) TR86–TR91.
[21] M. Han, D.F. Lawler, Interactions of two settling spheres: settling rates and collision efficiency, J. Hydraul. Eng. 117 (1991) 1269–1289.
[22] R. Di Felice, The sedimentation velocity of dilute suspensions of nearly monosized spheres, Int. J. Multiphase Flow 25 (1999) 559–574.
[23] P. Boogerd, B. Scarlett, R. Brouwer, Recent modelling of sedimentation of suspended particles: a survey, Irrig. Drain. 50 (2001) 109–128.
[24] T. Renganathan, K. Krishnaiah, Voidage characteristics and prediction of bed expansion in liquid–solid inverse fluidized bed, Chem. Eng. Sci. 60 (2005) 2545–2555.
[25] C. Boyer, A.-M. Duquenne, G. Wild, Measuring techniques in gas–liquid and gas–liquid–solid reactors, Chem. Eng. Sci. 57 (2002) 3185–3215.
[26] Z. Csikor, P. Mihatltz, L. Czako, J. Hollo, New interpretation of expansion in biofilm-coated particle fluidization, Appl. Microbiol. Biotechnol. 41 (1994) 608–614.
[27] T.E. Baldock, M.R. Tomkins, P. Nielsen, M.G. Hughes, Settling velocity of sediments at high concentrations, Coast. Eng. 51 (2004) 91–100.